LILI (Long-term Ice-field Levitating Investigator): Mars Aerial and Ground Explorer for Martian Polar Regions

Natasha Schatzman
Aerospace Engineer
NASA Ames Research Center
Moffett Field, CA, U.S.A

Michelle Dominguez
Aerospace Engineer
NASA Ames Research Center
Moffett Field, CA, U.S.A

Pascal Lee
Planetary Scientist
Mars and SETI Institutes
Mountain View, CA, U.S.A

Larry Young
Aerospace Engineer
NASA Ames Research Center
Moffett Field, CA, U.S.A

ABSTRACT

Exploration of Mars is currently underway by use of a rover and helicopter team. A hybrid ground/aerial vehicle concept that marries the respective strengths of rovers and rotorcraft for Mars exploration is presented in this paper. LILI (Long-term Ice-field Levitating Investigator) is a novel hybrid ground- and aerial-mobility concept vehicle proposed for exploration of the Martian polar regions. LILI combines episodic rotary-wing flight with primary ground-mobility-mode of a propeller-driven sled via an arrangement of three skis/runners and tilting proprotors. In this manner, the best of both worlds can be achieved for Mars polar exploration: rapid, obstacle-bypassing flight with low-power, efficient, longer duration -- and range -- sledding. LILI's propulsion system is based on solar-electric recharging of batteries. Consequently, periods of its air or ground movement are separated by periods of recharging. The overall project goal is to refine the vehicle and mission concept, while constrained within the current technology state of the art, and, leveraging the design heritage of the Ingenuity Mars Helicopter technology demonstrator. LILI's aerodynamic performance, flow interactions, and design characteristics, as well as potential mission profiles are suggested.

NOTATION

a	speed of sound (m/s)
c	chord length (m)
c_d	drag coefficient, $c_d = D/ (½ \rho V^2 c)$
c_l	lift coefficient, $c_l = L/ (½ \rho V^2 c)$
A	area of rotor, πR^2 (m^2)
A_s	area of skis (m^2)
C_T	coefficient of thrust, $\frac{T}{\rho A V_{tip}^2}$
D	section drag (N)
F_D	drag force of body (N)
F_F	friction force (N)
F_N	normal force (N)
F_W	force of LILI on Mars (N)
F_X	force in the x-direction (N)
g	gravity (m/s^2)
h	snow depth (m)
L	section lift (N)
M	Mach, $M = V/a$
N_b	number of blades
P	pressure (kg/m s^2)
R	rotor radius (m)
Re	Reynolds number
s	snow pressure (Pa)
T	temperature (deg K)
T	thrust (N)
V	velocity (m/s)
V_{tip}	tip speed (m/s)
α	angle-of-attack (deg)
ρ	density (kg/m^3)
ρ_s	snow density (kg/m^3)
$\theta_{1c,\ front}$	front rotor lateral cyclic pitch (deg)
$\theta_{1c,\ rear}$	rear rotor lateral cyclic pitch (deg)
$\theta_{1s,\ front}$	front rotor longitudinal cyclic pitch (deg)
$\theta_{1s,\ rear}$	rear rotor longitudinal cyclic pitch (deg)
$\theta_{0,\ front}$	front rotor collective pitch (deg)
$\theta_{0,\ rear}$	rear rotor collective pitch (deg)
$\theta_{S,\ front}$	front rotor shaft angle (deg)
$\theta_{S,\ rear}$	rear rotor shaft angle (deg)
σ	solidity, $\frac{N_b c R}{\pi R^2}$
μ	dynamic viscosity (kg/m s)
μ_f	coefficient of friction

Presented at the VFS Aeromechanics for Advanced Vertical Flight Technical Meeting, San Jose, CA, Jan 25-27, 2022.

INTRODUCTION

Mars exploration has been at the forefront of the planetary science community's research goals for many decades. Current NASA missions have aimed to explore the Martian terrain not only through rovers but, recently, also using uninhabited aerial vehicles (UAVs) (Refs. 1 - 3).

One of the key scientific goals from the Mars Exploration Program Analysis Group (MEPAG) –which helps NASA define its research priorities and missions – is understanding the processes and history of climate on Mars (Ref. 4). The LILI (Long-term Ice-field Levitating Investigator) project (first introduced in Ref. 3) would enable a closer look at the polar regions of Mars. For example, LILI could potentially enable the ability to drill in polar locations where a rover or UAV alone would not be able to reach. This fundamental hybrid ground/aerial vehicle concept could also be applied to terrestrial field science campaigns at the Earth's polar regions.

Due to the success of the Ingenuity Mars helicopter (Ref. 2), a new wave of aerospace innovation as applied to planetary aerial vehicles can be anticipated. LILI potentially helps realize a future vision to explore harsh terrains on Mars, where even the Ingenuity Mars helicopter and the Perseverance rover could not explore. This introduction to LILI identifies technical challenges to consider to further explore the scientific mysteries of Mars using a new generation of Mars rotorcraft that feature hybrid ground/air mobility.

PREVIOUS MARS POLAR REGION MISSIONS

Mars exploration has been ongoing since the 1960s (Ref. 5). Throughout the history of Mars exploration, missions have involved fly-bys, entry probes, orbiters, landers, and rovers. Due to Martian atmospheric and surface conditions, landing on Mars has proven to be especially difficult. Mars averages temperatures of -80 deg F and has one-third the gravity of Earth (Ref. 5). Missions to the Mars polar caps are even more difficult, with only a few successful missions thus far. NASA's Mariner 9 was the first to photograph the Martian poles in 1972. Then, in 2004, the European Space Agency's (ESA) Mars Express orbiter was able to detect evidence of water ice throughout the south polar cap. Later, in 2008, NASA's Phoenix lander touched down on the Mars northern plains known as Vastitas Borealis.

NASA scientists and engineers are particularly interested in studying Mars climate history by exploring the polar caps, i.e., the Planum Boreum (north) and the Planum Australe (south). Mars has a rotation axis that tilts at about 25 deg to its orbit around the Sun, and thus Mars has four seasons like the Earth. However, during the winter, the polar caps get colder and range from -153 to -243 deg F. The polar caps contain four geological units stacked on top of each other. The top stack is the seasonal ice cap, which is made of carbon dioxide, then the residual ice cap is made of water ice. Following the residual ice cap are the polar layered deposits, and these are made of thousands of thin layers of water ice mixed with dust. The last stack differs for each cap. In the south, there is the Dorsa Argentea Formation and in the north, there is the basal unit (Ref. 6).

In 1972, the Mariner 9 mission first photographed the Martian poles. Mariner 9's mission objectives were to map 70% of the Martian surface and study the temporal changes in the Martian atmosphere and on the Martian surface. According to NASA Space Science Data Coordinated Archive, images covering the entire planet were returned (Ref. 7). The Mariner 9 mission resulted in a global mapping of the surface of Mars, including the first detailed views of the polar caps.

In 1999, though lost at arrival, the Mars Polar Lander and the two Deep Space 2 probes were a part of NASA's New Millennium Program. Upon arrival, all communication was lost, and repeated efforts were made to contact the lander and the two probes, with no response. The two probes were designed to validate ten advanced, high-risk, high-payoff technologies (Ref. 7).

Then in 2004, the ESA Mars Express orbiter began science operations of the Red Planet. The objective of the Mars Express was to study all aspects of Mars, including its atmosphere and climate, and the mineralogy and geology of the surface and subsurface. The Mars Express had a high-resolution camera, a radar sounder, and other instruments - a total of seven instruments to complete its mission. The orbiter was able to send back 3D views of the Martian surface and discovered subsurface layers of water ice. One of the instruments was able to detect a large amount of water ice in the polar caps - enough to create a global ocean of 11-m deep if melted and evenly distributed across the planet. Also, the extensive plains of permafrost around the South Pole were unveiled (Ref. 7).

The 2008 Phoenix Mars Lander mission, which was part of the NASA's Scout program, successfully landed farther north than prior missions (Ref. 8 and 9). The Phoenix lander

carried a complex suite of instruments including a stereo camera, pressure sensors, tiny ovens, and a portable lab. Originally, planned for a 3-month mission, Phoenix lasted five months. During its mission, Phoenix dug into an ice layer near the surface and looked for evidence of life hospitality by using its robotic arm to collect samples of soil and ice. The selected samples were heated and chemical composition and other characteristics from the volatiles released were examined. The stereo camera provided range maps for the team to decide where it would dig, and the identification of local minerals was possible due to multi-spectral capability. Phoenix scanned the atmosphere of Mars up to 20 kilometers in altitude and obtained data on the formation, duration and movement of clouds, fog, and dust plumes.

LILI MISSION DESIGNS

Identification of mission locations are determined by previous missions and locations that aligns with the key scientific goals from the MEPAG. Two missions are described next, and the locations identified are from the 2008 Phoenix Mars Lander mission and attempted 1999 Mars Polar Lander/Deep Space 2 mission (Refs. 8 - 13). For each mission profile, the scientific mission will drive the vehicle mission requirements. The browser-based platform *Mars Trek* is used to visualize and identify locations of interests, especially the north polar cap (Refs. 14 and 15). Two missions are described and will be referred to as *Mission 1* and *Mission 2* throughout the paper. All noted distances (*) in missions are subject to change based on subsequent vehicle sizing calculations. Figure 1 and Figure 2 show the top view of the Mars polar region and Mercator projection map, respectfully, with *Mission 1* and *Mission 2* locations identified for LILI.

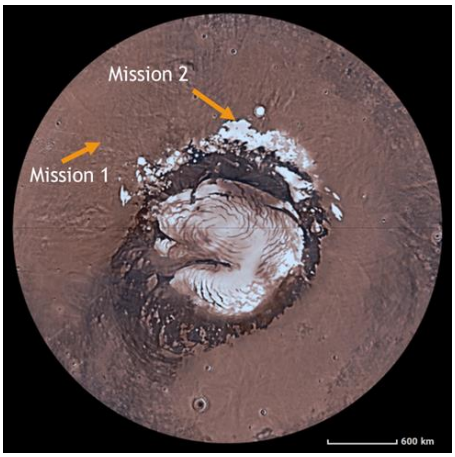

Figure 1. Top view of Mars north polar region with Mission 1 and Mission 2 locations identified for LILI.

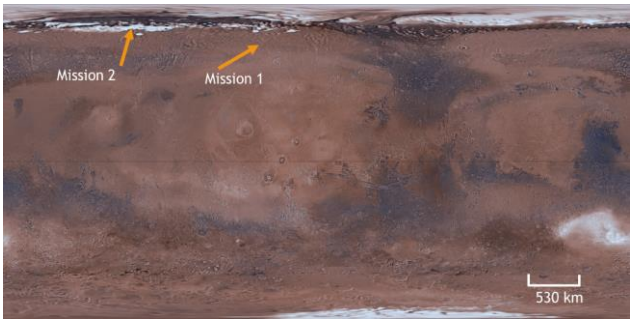

Figure 2. Mercator projection map of Mars polar region with Mission 1 and Mission 2 locations identified for LILI.

Mission 1: The first mission is set at an exterior polar region location of a Latitude of 67.5° N and Longitudinal of -125.7° W that is located in the Vastitas Borealis of Mars. This selected location is within the same proximity of the 2008 Phoenix Mars Lander mission. As shown in Figure 1 and Figure 2, *Mission 1* is also chosen due to its close external proximity of the polar region, without being fully engulfed in the harsh terrain of the upper polar cap. This location allows LILI to slowly traverse the unknown harsh terrain while utilizing LILI's unique design capabilities.

For this location, the majority of exploration will be by means of LILI in ground-mobility mode - rotors tilted and thrusting forward, propelling the vehicle forward on skis and/or wheel-skis. Due to obstacles such as uneven terrain and higher icy surface frictional forces, a wheel-ski design is suggested. *Mission 1*'s location is on the border of the polar cap, and because of this LILI could encounter both ice and non-ice terrain, where a wheel-ski configuration is more desirable for flexible transit over the unknown terrain.

The vehicle mission profile includes a maximum range (air and ground) of 10 km per vehicle charge, with a suggested route directed northward to explore a change in climate and terrain as the vehicle inches close to the polar caps, as shown in Figure 3. Once LILI has landed, LILI will climb 50 m and cruise 5 km, descend 50 m, and explore for 5 km on the surface while performing scientific experiments. Depending on power, LILI will charge either before or after the ground exploration begins. A depiction of *Mission 1* is shown in Figure 4. These large distance "hops" would accommodate change in terrain and climate versus latitude direction. Note that these flight leg ranges – for both *Mission 1* and *Mission 2* represent initial "ideal" mission design targets and will be subject to additional scrutiny and realism with respect to vehicle design sizing analysis presented later in the paper.

In terms of scientific exploration, since the vehicle mission profile includes a latitudinal exploration, an ice drill is suggested to sample along the mission to further understand Mars as LILI moves closer to the polar cap. The strength of the icy surface is not only dependent upon temperature, but also water content, where penetration strength and choice of

drill system will need to be further investigated (Refs. 16 and 17). This drilling procedure will consist of breaking the formation and removing the drilled cuttings. Use of an ice drill will reveal further information about the formation of Mars.

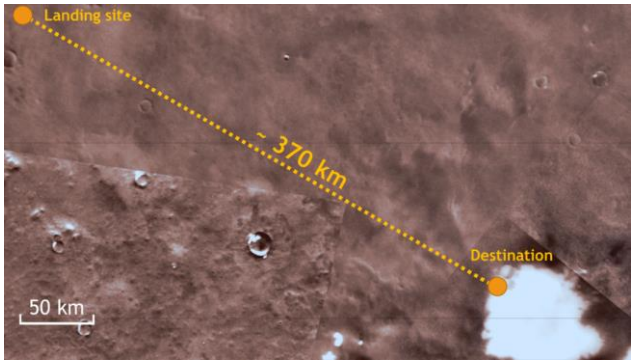

Figure 3. Mission 1 landing and destination location.

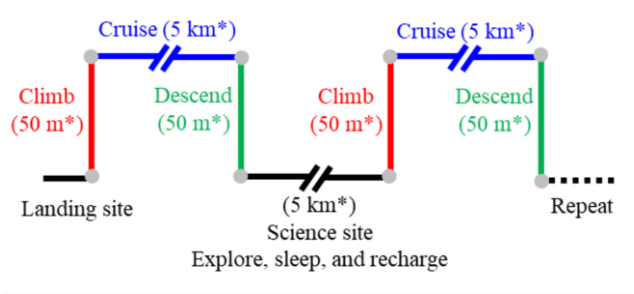

Figure 4. Mission 1 design mission (*distances subject to change based on results from sizing iterations).

Mission 2: For the second mission, an interior polar region is suggested at a Latitude of 76° N and Longitudinal location of 170° W. This location is based on the previous mission of the 1999 Mars Polar Under/Deep Space 2. *Mission 2* will be operating further into the polar cap of Mars compared to *Mission* 1.

Due to the harsh terrain, hover and forward flight is suggested for areas that are difficult to transit with skis. Though *Mission 2* is further within the polar region, the mission can also utilize the wheel-ski configuration for ground navigation.

Mission 2's mission profile includes a lateral and longitudinal exploration within a suggested area of approximately 15,000 km^2. The suggested area was only an attempted mission and so little is known about the terrain. The landing site and area of exploration is shown in Figure 5, where four stations are identified as areas of interest to explore. *Mission 2* comprises into 3 legs, as shown in Figure 6.

Mission 2 leg 1 (Figure 6 a)), starts at station 1 at the landing site where LILI will charge and prepare for the first leg. LILI will climb 25 m, cruise for 10 km, descend 25 m, and recharge. Next, LILI will climb 25 m and cruise for 5 km and descend (<25 m) into the icy canyon. While in the canyon, LILI will recharge and begin to explore the canyon using both LILI's hovering capabilities and wheel-ski configuration for 5 km to reach station 2.

For *Mission 2's* leg 2 (Figure 6 b)), starting from station 2 LILI will recharge and climb out of the canyon and cruise 10 km then descend to the surface to recharge. This sequence will repeat two more times until LILI has reached station 3. While at station 3, LILI's wheel configuration will be utilized along with LILI's hovering capabilities to maneuver around the terrain.

Finally, for the last leg (Figure 6 c)) starting at station 3, LILI will recharge and climb and cruise for 10 km three times until reaching station 4, where LILI will perform further scientific experiments.

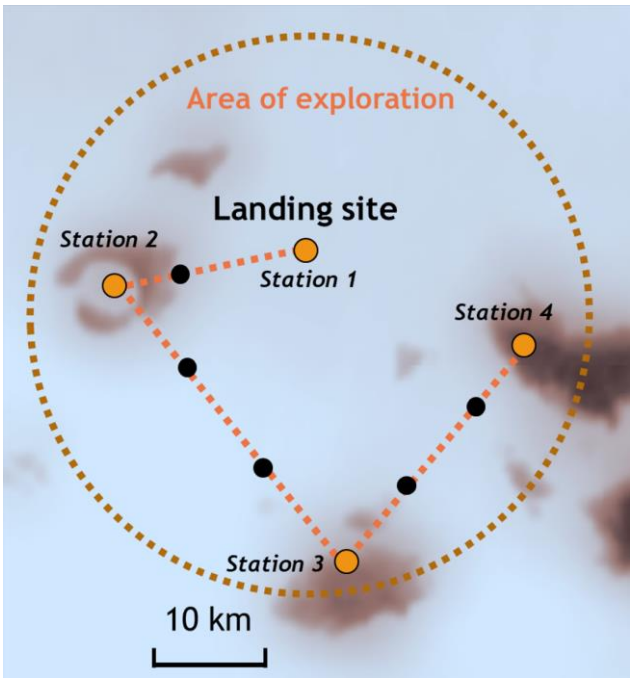

Figure 5. Mission 2 landing site and area of exploration map.

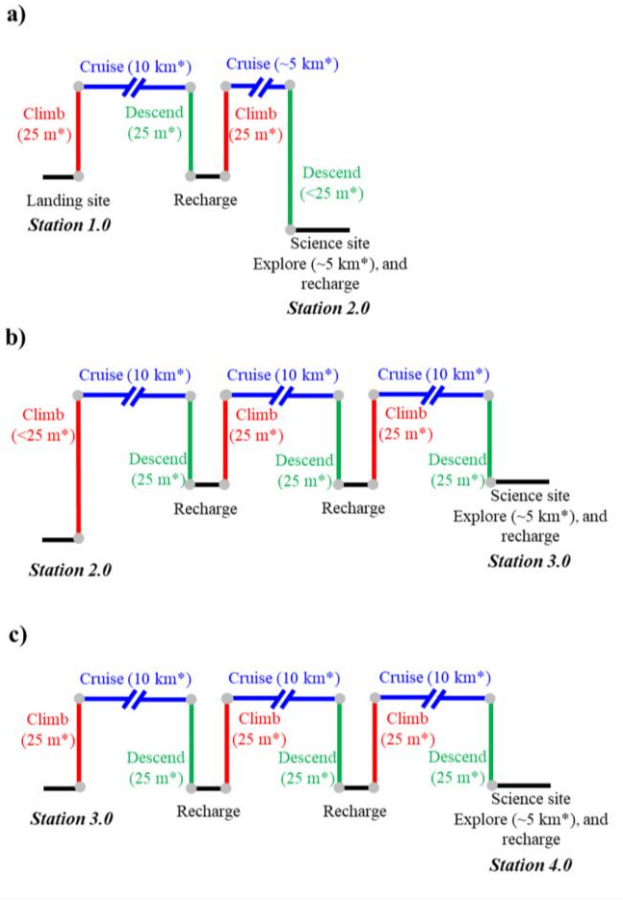

Figure 6. Mission 2 design mission for a) leg 1, b) leg 2, and c) leg 3 (*distances subject to change based on sixing results).

LILI VEHICLE DESIGN SPECIFICATIONS, PROCESS, AND INITIAL SIZING

Aspects of LILI design specifications, process of design, and initial sizing are discussed next. In particular, the unique challenges and analysis required for hybrid air and ground mobility will be highlighted, including considerations for using skis/runners for ground mobility on snow or icy surfaces.

Design Specifications

LILI's original design consists of three skis arranged with two skis ahead of one trailing ski. The forward skis support a single four-bladed rotor, with the trailing ski supporting another four-bladed rotor. The two rotors are connected via a shaft and/or truss-structure for fixed-frame stiffness and (possible) rotor azimuthal synchronization. The rotors' variable-pitch (rotor collective and cyclic control) enables not only control of forward direction, but also allows for other desired. In the flight-mode, rotor axes vertical, the rotors act in concert as a tandem helicopter-like configuration. In ground-mode, the rotors are tilted forward ninety degrees and the thrust of the now (widely spaced rotor-to-rotor) coaxial rotors is aligned with the horizontal axis and the rotors provide the propulsive force to drive the LILI vehicle across the ground/surface on its skis/runners (or some combination of skis and free-spinning wheels). The LILI ground-mode on the Martian polar icefields is analogous to an airboat on water on Earth. Figure 7a) shows LILI in hover in its flight-mode configuration isometric view. For the hover configuration the two rotors are rotated vertically and thrusting upward (positive z direction). This rotor tilt configuration would allow for vertical take-off and landing in harsh polar regions, where a rover would not be able to navigate. For ground-mode horizontal travel, the rotors provide forward thrust, while the skis/runners are used to overcome the icy terrain, see Figure 8a) isometric view. This ground-mode configuration minimizes power compared to using a UAV, because it does not have to provide lift by means of the rotors to carry the full weight of the vehicle to travel and explore.

Table 1. LILI initial rotor specifications.

number of rotors	2				
number of blades	4				
radius (m)	0.85				
height of front rotor from ski (m)	1.11				
height of rear rotor from ski (m)	1.11				
rotor-rotor hub separation (forward flight) (m)	1.94				
front rotor rotational direction	counterclockwise				
rear rotor rotational direction	clockwise				
chord					
r/R	0.09	0.25	0.5	0.75	1
chord/R	0.12	0.17	0.16	0.16	0.11
twist					
r/R	0.09	0.25	0.5	0.75	1
twist (deg)	11.88	9	4.5	0	-4.5

LILI takes advantage of pre-existing Ingenuity Mars Helicopter and Mars Science Helicopter (MSH) rotor and other hardware design heritage and validated rotorcraft sizing analysis work as starting points (Refs. 2 and 12). A complete list of initial rotor specifications is provided in Table 1. The number of rotors and blades, radius, chord, and twist distribution are provided. Each of the two rotors has four blades with a 0.85-meter radius, a nonlinear chord

distribution, and a linear twist distribution. The spreadsheet-based sizing analysis, as detailed later in the paper, will increase the overall size of the vehicle from these initial starting point numbers. The front rotor rotates counterclockwise, while the rear rotor rotates clockwise. The airfoils used for the LILI RotCFD analysis are drawn from Ref 10.

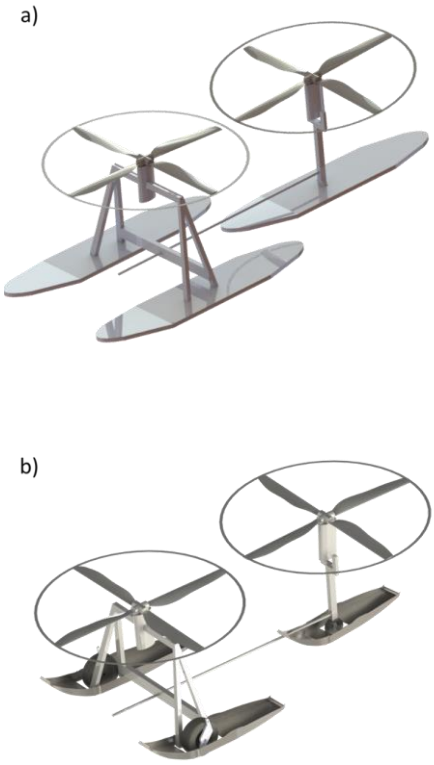

Figure 7. LILI concept vehicle in hover configuration a) original, and b) with ski plus wheel isometric view.

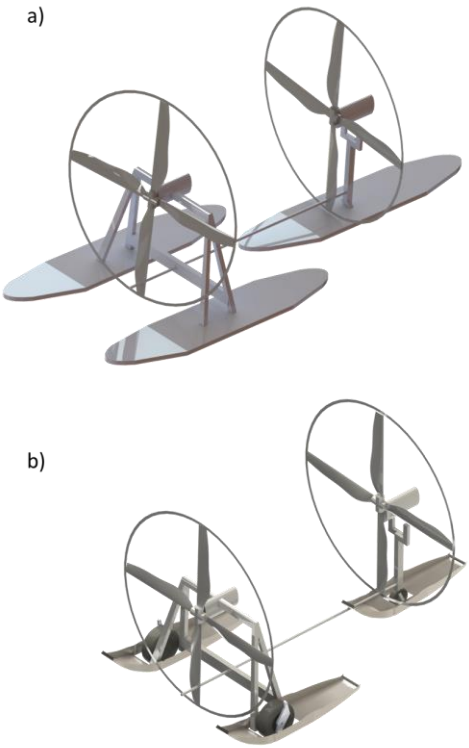

Figure 8. LILI concept vehicle in forward flight and ground exploration configuration a) original, and b) with ski plus wheel isometric view.

The propulsion system is based on solar-electric recharging of batteries. Consequently, periods of LILI movement are separated by periods of recharging. The reduced solar flux of the Martian polar regions will require careful consideration of the duration and the active seasonal phase of the mission. To successfully navigate the Martian polar regions while also maintaining sufficient power, alternative ground mobility elements must be considered as well. Using propeller-driven propulsion for even the ground mobility mode minimizes wheel-traction concerns when traversing icy terrain and using low friction for maneuverability. Finally, if the terrain becomes too rough or otherwise impassible by skis, the vehicle can tilt its rotors vertically and takeoff, fly (as a tandem-helicopter-like configuration) and land in a more benign area.

Unique design aspects of Wheel-Skis

To tackle the icy harsh terrains of Mars polar caps, the initial ski design was further developed to include a wheel plus ski ("wheel-ski") configuration. Though LILI has the capability to use rotors to travel close to the surface of mars via hover, the wheel-ski design will enable deeper exploration by staying closer to the surface of Mars.

The wheel-ski design, configuration will affect the operation and performance of LILI in many ways, including its takeoff, landing, and flight operations. Typically, ski planes or aircraft with a wheel-ski design land on frozen or

snow-covered terrain but can be designed for numerous forms and conditions of snow and ice. For LILI, the combination ski configuration allows for the use of skis on snow and ice, but also the use of wheels on non-snow terrain.

Two types of combination skis are explored: the retractable ski and the penetration ski. The retractable ski type allows the ski to be extended into place or retracted, depending on the operations, where a hydraulic pump or crank is used. With the penetration ski design, the wheel extends partially below the ski. This type of ski stays extended while operating on snow and non-snow terrain.

For the design of the wheel-ski, the various types and slopes of terrain are considered. Tire parameters such as diameter, width, tread, mass, turn radius, loading, placement, shaft axis, mounting, quantity of tires where considered as well if the system would have a passive or active tire deployment.

The wheel-ski is shown in Figure 7b) and Figure 8b). The wheel-ski is designed to be a passive retractable design that would enable the wheels to deploy/unlock as needed. Furthermore, the design considers stowage options (to fit within the entry, descent, and landing (EDL) aeroshell) and will be discussed in the aeroshell portion of this paper.

Packaging/stowage issues of the robotic mobility system into a Pathfinder-class aeroshell was considered early in this paper's study. The overall project goal is to arrive at a near-term NASA Mars mission proposal – thus requiring high technology readiness levels of the key systems, achievable within the current technology state of the art and leveraging significantly from the design heritage of the Ingenuity Mars Helicopter technology demonstrator.

Design Process

Due to LILI's unique areas of exploration and design capabilities an example design flow chart is provided to account for the unconventional parameters not seen in common and current designs. To design a mission for LILI, an example design flow chart is presented in Figure 9.

A mission is first defined, followed by a list of mission parameters that includes, but is not limited to: charge time, length of mission time and speed per flight condition, and operational configuration (ground or arial flight). At this stage, an estimate of type of terrain should be identified, including type of ice or snow.

While defining ground exploration many factors should be considered, for example: terrain variation, maximum contact pressure of skis and wheels, and minimum thrust for skis to slide on land. For maximum contact pressure of skis and wheels, the larger the contact area of a ski or snowshoe allows more force to be distributed over a large area to slide across the snow and not sink. For LILI, the larger the contact area, the greater weight of LILI can be. Other factors effect limitations such as stiffness, shape, and type of mounting of the skis. Furthermore, the type of snow is also a factor, whether you have powdery or hard packed snow will determine how large the contact area of the skis should be for maximum allowable pressure on are of skis.

For LILI not to sink in the snow the area of the skis (A_s), snow or terrain variation, and mass of the vehicle (m) times Mars gravity (g) or force (F), must be considered. The pressure on the snow from there area of the skis and weight of the vehicle must not be greater than the snow pressure, otherwise LILI would sink. Using the snow depth (h), density of the snow (ρ_s), and acceleration of gravity on Mars, the snow pressure (s) can be calculated, see Eq. 1 (Ref.11). The pressure from the weight of the vehicle is calculated using Eq. 2. The pressure on the snow (P) must be less than the snow pressure (s), see Eq. 3.

$$s = h\rho_s g \tag{1}$$

$$P = \frac{F}{A_s} \tag{2}$$

$$s \geq P \tag{3}$$

For LILI to move forward, thrust from the rotors must overcome the friction force of the weight, terrain, and aerodynamic drag. Using the mass of the vehicle (m) times Mars gravity (g), coefficient of friction of the snow (μ), and angle slope of the terrain (θ), the thrust to overcome the external forces can be computed. A free-body diagram of the rear rotor traveling uphill is shown in Figure 10a). For LILI to travel upward, the forces F_x (horizontal force), F_F (frictional force), and F_D (drag force), must be less than the force of thrust, F_T. For LILI to travel backwards on level ground (Figure 10b), the F_F and F_D must be less than a negative thrust vector. Turning LILI requires a cyclic control input that would move the thrust vector along the right side of the rotor, as shown in Figure 10c), where the side and top view provided show a thrust vector located on the right side of LILI's rear rotor.

After the constraints are met, payload requirements can be defined. The payload weight along with the weight of GNC sensors/avionics are considered dependent on the need for ground and flight phases of the missions. Furthermore, an estimate weight of the skis and or wheels, mounting support structure, and deployment actuators are calculated to determine the maximum contact pressure, where weight is not limited to science equipment, skis, and other structures.

Once the mission profile, constraints, and payload are defined, the energy required can be determined to complete the mission profile and size the battery mass.

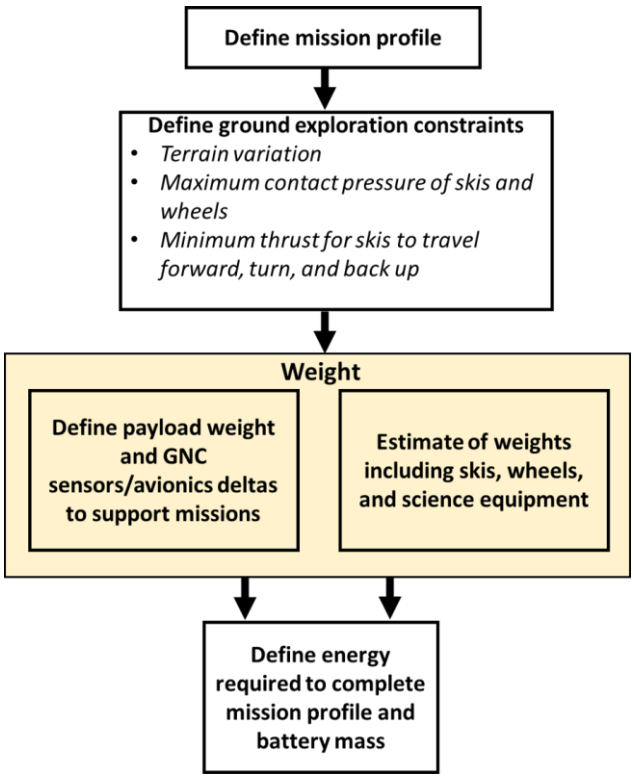

Figure 9. LILI design flow chart.

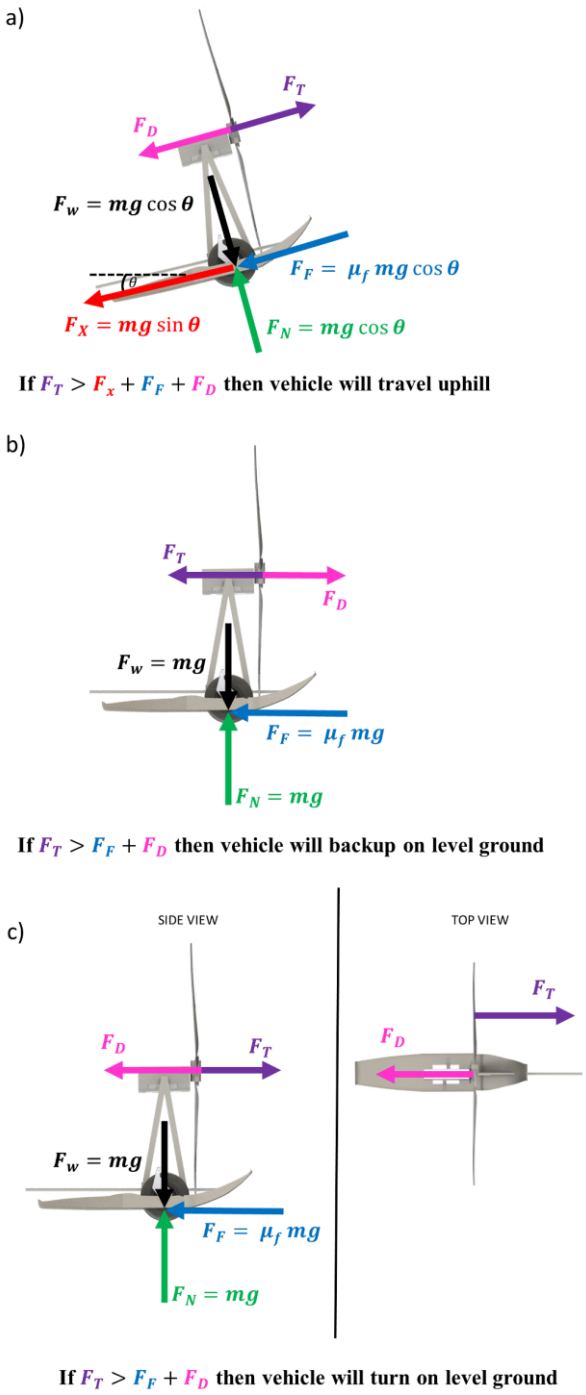

Figure 10. Free body diagram of LILI a) rear rotor and ski traveling up hill, b) rear rotor on level ground reversing, and c) rear rotor turning on level ground.

Vehicle sizing

The sizing of LILI leverages previous Mars rotorcraft sizing work by Johnson et al. (Ref. 12) that provided a conceptual design process along with identified constraints and key parameters for initial estimates of weight and performance based on the capabilities of the Mars Helicopter. From this work, a spreadsheet was developed to size a

helicopter for Mars missions. The spreadsheet provides an initial estimate of the aircraft size and was calibrated to the weight and power of the Mars Helicopter. Simple models for rotor performance, motor and battery efficiency, and component weights were implemented. These simple aeroperformance models will be updated by computational fluid dynamics predictions made by the RotCFD software tool.

Initial sizing efforts used the existing spreadsheet from Johnson et al. (2012) by first accounting for the tandem-like configuration of LILI. To account for the ski and wheels for ground exploration missions, various key parameters were identified and implemented into the spreadsheet that include (but are not limited to):

- Number of skis and wheels
- Maximum contact pressure of skis on snow/ice (ski area)
- Dynamic coefficient of friction from skis
- Static coefficient of friction
- Terrain grade (slope of terrain)
- Ski and wheel gross weight
- Truss rotor support between two tandem rotors/ radius
- Truss support between two tandem rotors length
- Collapsible/deployable rotor nacelle supports gross weight

All listed parameters are used to calculate LILI's ground transit requirements in the updated spreadsheet. As shown previously in Figure 10, the addition of skis/wheels must be taken into account to ensure that thrust from LILI's rotors overcome the weight, friction from the skis/wheels, and the drag of vehicle. An example of required thrust for LILI in ground transportation mode is shown in Eq. 4, where T is the total thrust from both rotors.

$$T = \mu_f mg \cos\theta + F_D \tag{4}$$

As a first attempt, with the use of the modified spread sheet (Johnson et al. (Ref. 12)), a mission consists of the following legs: 1) takeoff, 2) vertical climb to altitude, 3) fly to site, 4) hover at site, and 5) ground transits. A gross weight study was performed on a variation the leg 3 distance of 500, 750, and 1,000 m and ground transit (leg 5) time from 5 to 30 min, including a comparison of temperature for -100 and -200 deg F (see Figure 11). For this initial study, take-off time was set to 30 s, the vertical climb to desired altitude was 200 m, and hover at site was set to 1 min. Calculations reveal a minimal increase in gross weight for a fly-to-site variation of 500 to 100 m (less than 1-kg difference), with a larger increase in weight when the ground transit is increased for each 5-min increment (greater than 1 kg per 5-min increase). A study in temperature variation was performed revealing a difference of approximately 2 kg when the temperature was decreased from -100 to -200 deg F at a ground transit of 5 minutes. Temperature variation does not affect the gross weight as much when the ground transit time is increased. This study revealed that temperature should be a key parameter in the design processes and that the flight time is less sensitive compared to ground transit.

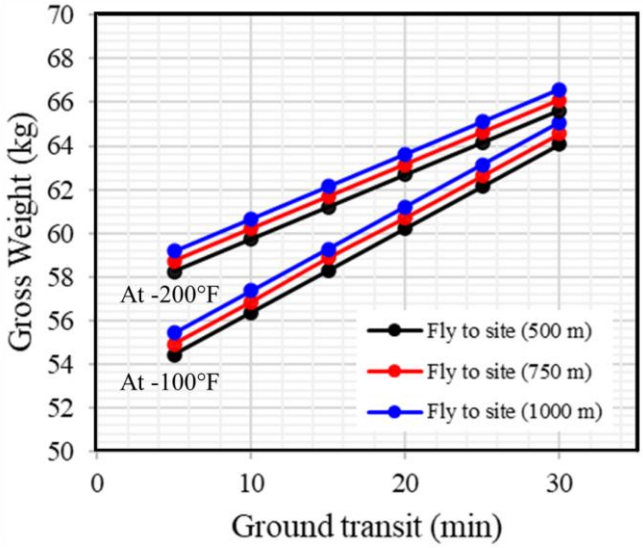

Figure 11. Gross Weight verses ground transit for variation in fly to site distance and temperature.

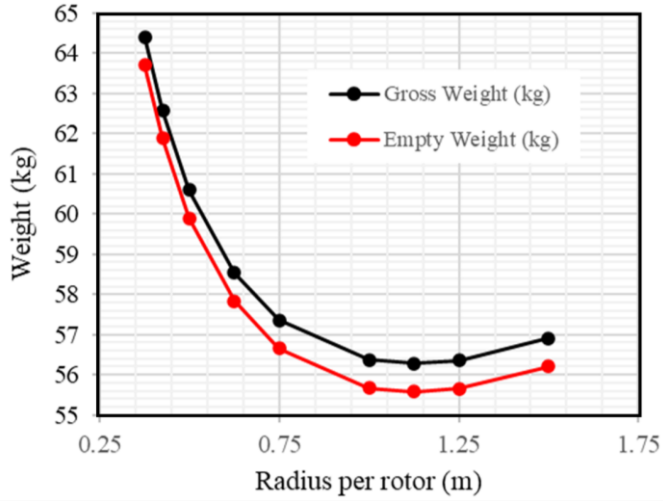

Figure 12. Gross weight and empty weight for various rotor radii.

A summary output from the updated sizing spread sheet is provided in Table 2 for a mission definition with a takeoff of 30 s, vertical climb to an altitude of 200 m, flight to a site that is 500 m away at a speed of 30 m/s, hovering at site for 1 min and ground transit for 10 min. The ground transit calculations include a positive 5-deg incline, as LILI could encounter high slope terrain. Calculations revealed a total gross weight of 56.36 kg, which includes the weight of the skis and wheels. Furthermore, calculations revealed a radius of 1.25 m, which is an increase from the original design as shown in Table 1. Design points include a thrust of 215 N and hover figure of merit (FM) of 0.5.

A study was performed on gross weight and empty weight versus rotor radius - see Figure 12 - at a temperature of -100 deg F. The mission definition is given in Table 2. As the rotor radii are increased, the total gross and empty weight also decrease due to the increase in thrust up until the radius = 1.00 m. As the rotor radius is increased past 1.25 m, the gross and empty weight begin to increase again. These curves should be taken into consideration when designing to identify minimum weight.

To further improve the sizing spreadsheet results, more information pertaining to mission locations is needed, including density, temperature, speed of sound, viscosity, and kinematic viscosity at the northern polar regions of Mars. Accounting for vehicle download in hover and forward flight due to the skis is also a suggested update to the spreadsheet. Furthermore, it is desired to have more precise weights and friction coefficients to determine more exact calculations.

STORAGE AND DEPLOYMENT

The processes of how LILI will collapse to minimize storage area to fit inside the aeroshell and successfully deploy to begin exploration are discussed next. Figure 13 shows the deployment of LILI on the Martian surface via parachute. For storage, LILI consists of two sections which connect at each end with a rod that goes through the model. Both sections containing the skis and rotors slide inward towards each other on the rod when LILI is in its collapsed stage. For deployment, a sky crane is used which covers the collapsed model that is stored under the sky crane. Once LILI is collapsed and stored, LILI and the sky crane will be place inside the aeroshell.

Table 2. Summary example of sizing output calculations for LILI.

Mission Definition		
takeoff	0.5	min
vertical climb to altitude	200	m
fly to site at 30 m/s	500	m
hover at site	1	min
ground transit	10	min
Weight break down summary		
empty weight*	55.66	kg
fixed useful load	0.2	kg
payload	0.5	kg
gross weight	56.36	kg
*includes, but not limited to structure, fuselage (skis, wheels, etc.), propulsion, systems and equipment		
Rotor specifications and design points		
number of rotors	2	
number of blades	4	
radius	1.25	m
chord	0.465	m
solidity (σ)	0.946	
RPM	1280	
M_{tip}	0.7	
C_T/σ	0.11	
design thrust	215.3	N
disk loading	43.9	N/m^2
hover FM	0.5	
motor power	30863	W
Reynolds number	73340	

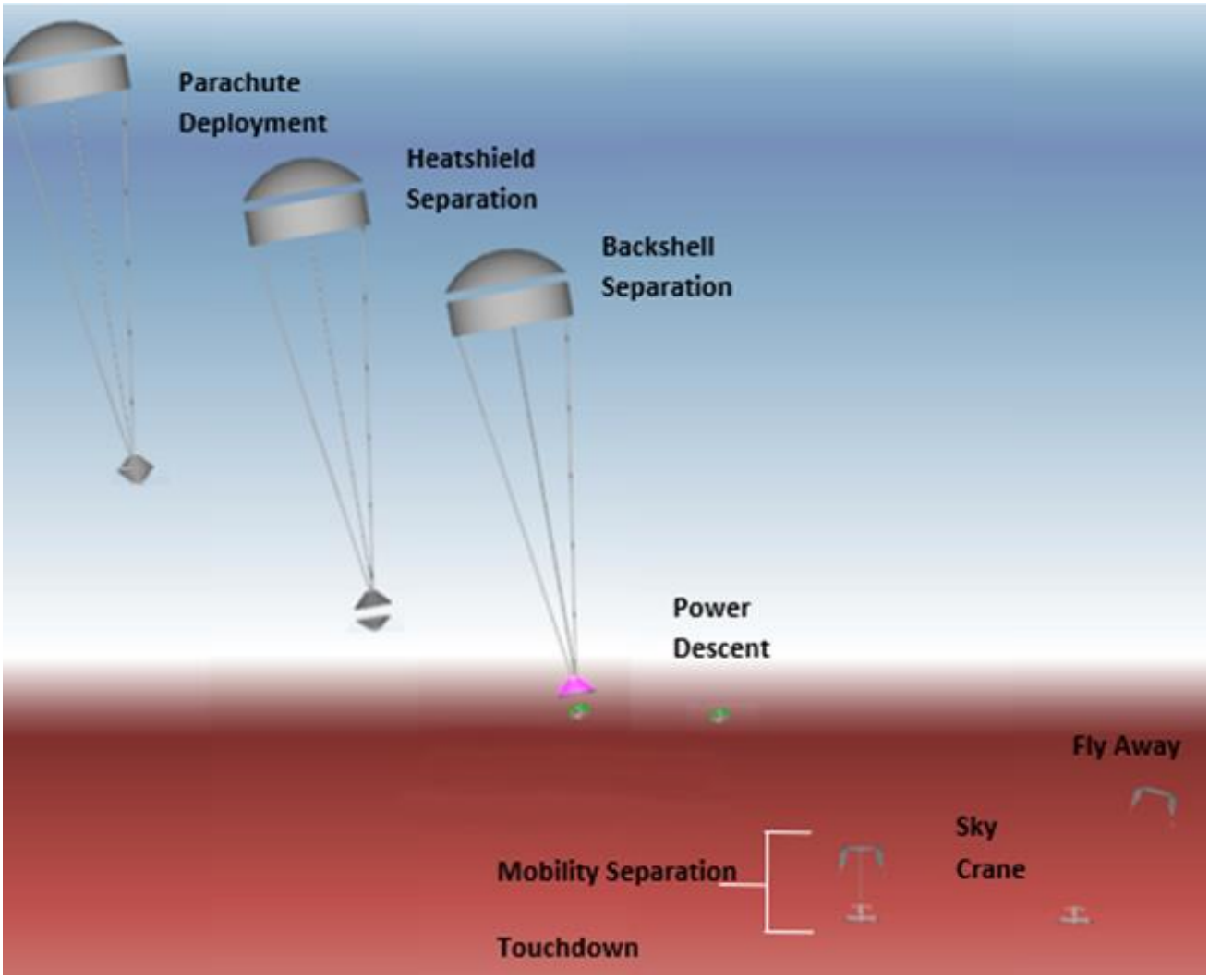

Figure 13. Deployment of LILI on Martian surface via parachute.

Storage

LILI will be packed inside an aeroshell, consisting of a backshell and heat shield. The aeroshell serves as a protective cover during the long voyage to Mars. The aeroshell's main purpose is to protect the sky crane and LILI from the heating of entry into the thin Martian atmosphere (Ref. 18).

Aeroshell design

The aeroshell for LILI as shown in Figure 14, is made up of two main parts, the heat shield and the backshell (Ref. 18). The heat shield will protect the sky crane and LILI from the heat from entry into Mars and aerodynamically acts as a first brake. The backshell will carry a parachute and other components which will be used at later stages of entry, descent, and landing.

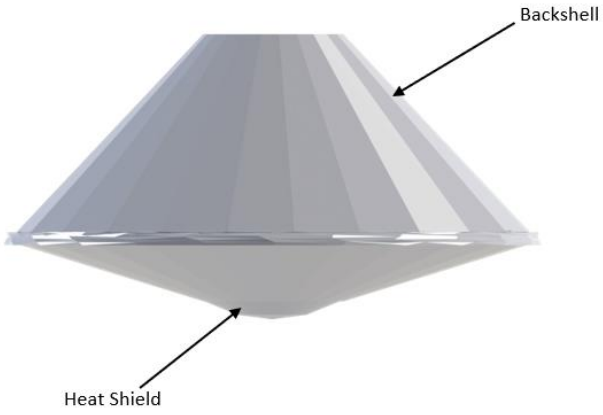

Figure 14. Aeroshell for LILI.

Collapsible stages

LILI will have skis/wheels and collapsible/expandable telescoping tubes and/or truss structures for the fixed-frame (nonrotating) vehicle structures that will fold up during flight. Figure 15 a) shows LILI in its fully collapsed configuration and stored under the sky crane. In Figure 15 b) the sky crane extends and pulls away from the model. Then, in Figure 15 c) the model begins to expand and both sections slide outward, away from each other and to opposite ends. Finally, the model expands to its full state and locked in place and the rotor and blades go to forward flight position where LILI is ready to be deployed (Figure 15 d).

Deployment

Landing LILI happens in a number of EDL stages, as depicted in Figure 15. In many ways the proposed approach is consistent with the skycrane approach used for both the Curiosity and the 2020 Perseverance rover missions (e.g. Ref.19). After the aeroshell slows down as it approaches the Mars surface, the parachute is deployed which is attached to the aeroshell; in turn, the aeroshell contains the skycrane and the collapsed LILI vehicle. Following the deployment of the parachute, the heat shield separates along with the parachute and separates away. Finally, the skycrane maneuver is initiated at the final descent speed to land LILI safety on the surface of Mars. The key difference using a skycrane approach for LILI is that the mass of LILI is significantly lower than that of the rovers, however, the volumetric size of the stowed LILI is comparable to that of the stowed rovers.

Skycrane

The proposed skycrane for LILI consists of four thrusters, with two thrusters on each side of the top of the aeroshell along with deployable legs/support-arms on each side to stabilize LILI as it is lowered by a tether(s) from the hovering skycrane. The skycrane gives the ability to safety deploy LILI onto the surface of Mars with minimal external movement and is anticipated to be more robust of a deployment approach that alternatives. Use of the skycrane has various advantages, but also some draw backs. Draw backs include a complicated control and stability system for the skycrane platform. Furthermore, there is limited ability to experimentally test the skycrane at full scale under Mars-like conditions.

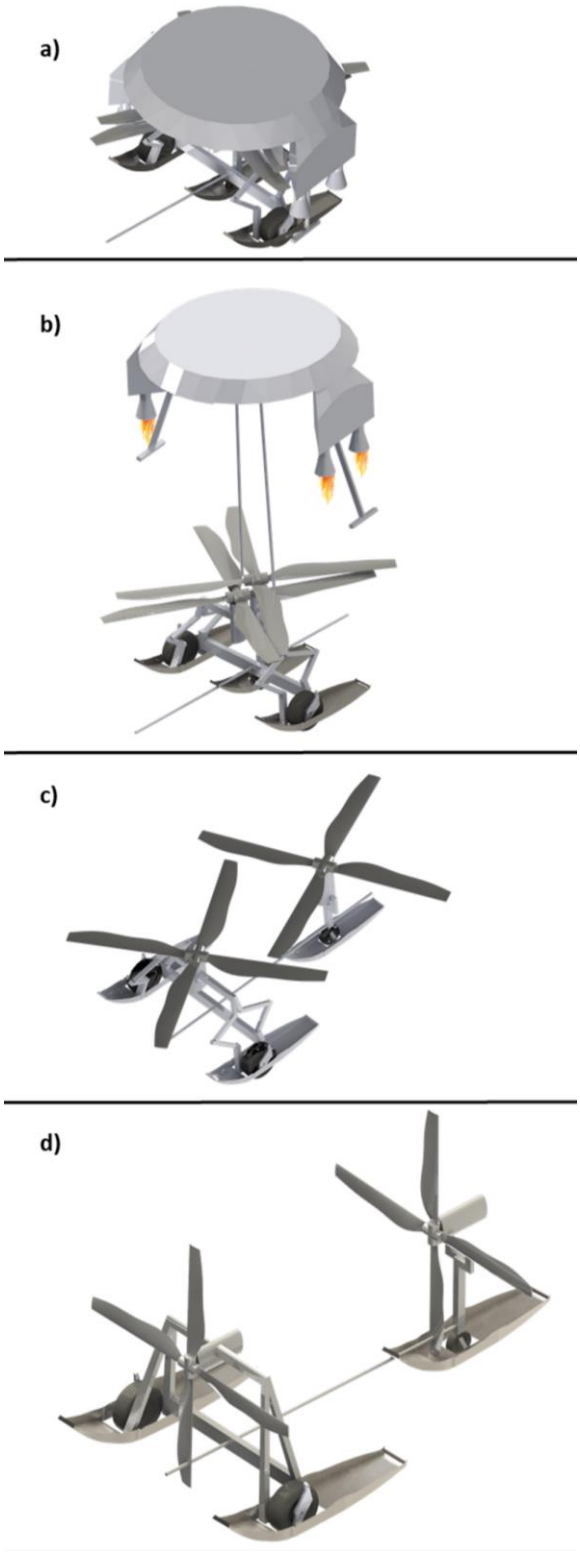

Figure 15. Deployment of LILI from a) collapsed configuration and stored under the sky crane, b) mobility separation, c) horizontal separation of two rotors and d) final ground exploration configuration.

AERODYNAMIC PERFORMANCE AND CONTROLLABILITY ASPECTS OF LILI

Due to LILI's unique vehicle configuration, various aerodynamic, performance, and control input studies under different operational modes and conditions were performed. Studies included hover, ground mobility, and forward flight flow field analysis, Mars versus Earth wake flow field. The program Rotor Unstructured Navier-Stokes (RotUNS) was used to calculate the flow field and performance of LILI and explore LILI's response to control inputs. All calculations are computed using LILI's original ski design, as shown in Figure 7a) and Figure 8a).

ROTOR UNSTRUCTURED NAVIER-STOKES (RotUNS)

Rotor Unstructured Navier-Stokes (RotUNS) operates within the RotCFD Integrated Design Environment (IDE) (Ref. 20 and 21). RotUNS is one of several flow solvers within RotCFD, which also includes a geometry module, a semi-automated grid generation module, a rotor module, and a flow visualization and analysis module, all integrated in one environment. Within the RotCFD IDE, grid generation and problem setup are quickly executed, facilitating parametric sweeps of rotor conditions and problem geometry. RotCFD balances ease of use and practical resource constraints with an accurate physical representation of the global flow field. Within the RotUNS environment, the following nominal Earth and Mars conditions that are used in this study are shown in Table 3. The air density on Mars is approximately 1% of Earth. Earth consists of primarily of nitrogen and oxygen ($N_2 + O_2$), while Mars atmosphere consists of primary carbon dioxide (CO_2). Due to the low temperatures and gas properties of carbon dioxide on Mars, the speed of sound is lower compared to Earth.

The flow properties used for the illustrative RotCFD predictions are: an atmospheric density of 0.01kg/m^3 (at the lower-end of Mars surface atmospheric densities); a static temperature of 214 Kelvin; a specific heat ratio of 1.29; a dynamic viscosity of 1.08E-005; a static pressure of 584 Pascal. The 'realizable $\kappa-\varepsilon$ turbulence model' was used for the flow field predictions. The rotor configuration is based on the chord, twist, and airfoil distributions of the 17 kg Mars Science Helicopter configuration described in Ref. 12, and uses the compressible, low-Reynolds number circular-arc airfoils describe in Ref. 10. The rotors were set at a uniform collective of ten degrees and a tip speed of 183 m/s for hover and forward flight; for this initial work the rotors were untrimmed (either by collective or tip speed) for hover and tip speed. Only the RotCFD 'steady rotor option' was used to model the rotors (distributed momentum sources to describe an actuator disk). The body refinement is eleven (body-fitted) and the rotor refinement is nine. Three nested grid refinement boxes were used: the outer, larger box of a grid refinement of five, an intermediate, mid-size box of refinement six, and a smaller, inner refinement box of refinement seven. The overall gridding for these initial results was relatively coarse: 898,355 cells, see Figure 16. Finally, relative coarse time step of 1000 time steps for 10 seconds of simulated time was used for these initial predictions. All cases were run with OpenCL GPU parallel processing. Future work can model the rotor with the RotCFD 'unsteady rotor option' (i.e. lifting line rotor blade modeling) as well as higher grid refinements and using the collective/cyclic trim option for the LILI configuration in tandem-helicopter-mode for edgewise forward flight. Each computational simulation in RotCFD was not trimmed but set to a specific control input. Front and rear rotor shaft settings ($\theta_{S,\ front}$, $\theta_{S,\ rear}$) and collective pitch ($\theta_{0,\ front}$ $\theta_{0,\ rear}$) is noted for all simulations. Use of lateral and longitudinal cyclic pitch control is denoted as θ_{1c} and θ_{1s} respectively, for both the front and rear rotors. Results presented from RotCFD are intended to be a high-level first look into the flow field of LILI for various flight and ground regimes.

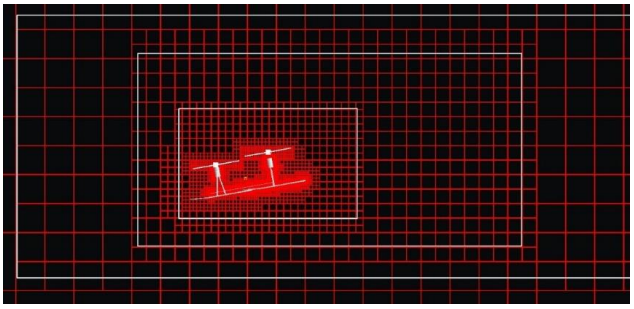

Figure 16. Gridding and refinement boxes for LILI simulation in RotCFD.

Table 3. LILI atmospheric conditions on Earth and Mars.

	Earth ($N_2 + O_2$)	Mars (CO_2)
Temperature (K)	288	214
Density (kg/m^3)	1.225	0.0117
Gas constant (J/Mol K)	287	189
Specific Heat Ratio (J/K kg)	1.4	1.29
Dynamic Viscosity (kg/m s)	1.7894 x 10^{-5}	1.08 x 10^{-5}
Pressure (kg/m s^2)	101325	584
Speed of sound (m/s)	340.3	233.1

Hover, ground mobility and forward flight wake analysis

Each primary flight/mobility condition is explored in RotCFD for hover, ground exploration, and forward flight as seen in Figure 17 through Figure 19, respectively. The RotCFD velocity magnitude iso surface flow field for the

LILI hover configuration reveals that the area of skis needs to be tailored to maximize the hover capability, e.g. skis too large will decrease hover efficiency due to the download of the skis from the rotor wake (Figure 17). The ground mobility flow field simulations reveal that the rotor wake from the forward rotor is ingested in the trailing rotor (Figure 18). LILI in forward flight with the rotors tilted forward and a 20 m/s velocity vector reveals minimal wake impingement on the front skis with a large amount of the wake hitting the single rear ski (Figure 19).

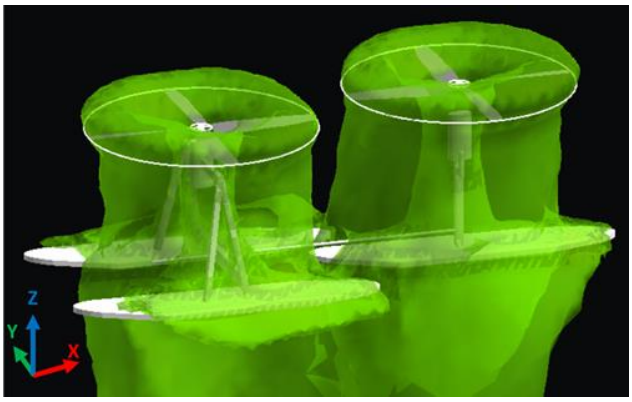

Figure 17. LILI in hover mode: velocity magnitude iso surface flow field prediction ($\theta_{S,\,front}$ = 0°, $\theta_{0,\,front}$ = 10°, $C_{T,\,front}$ = 0.0253, $\theta_{S,\,front}$ = 0°, $\theta_{0,\,rear}$ = 10°, $C_{T,\,rear}$ = 0.0260).

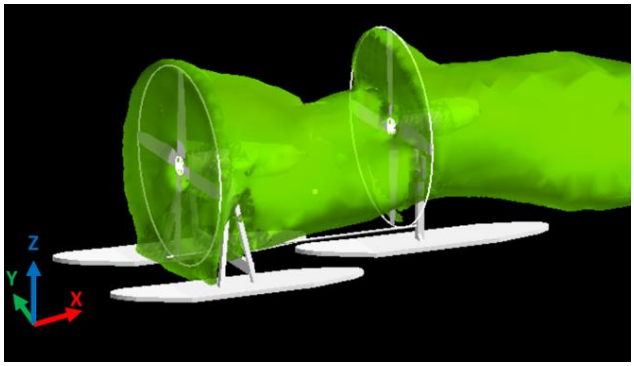

Figure 18. LILI in ground mobility mode: velocity magnitude iso surface flow field prediction ($\theta_{S,\,front}$ = 90°, $\theta_{0,\,front}$ = 10°, $C_{T,\,front}$ = 0.0315, $\theta_{S,\,rear}$= 90°, $\theta_{0,\,rear}$ = 10°, $C_{T,\,rear}$ = 0.0281).

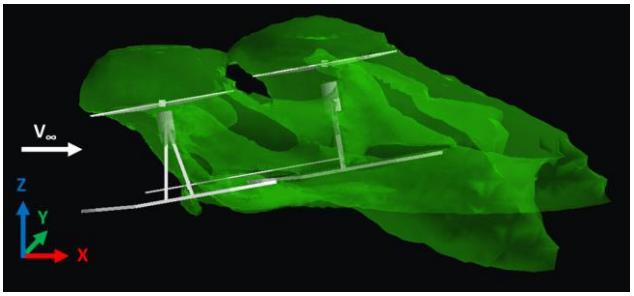

Figure 19. LILI in forward flight mode: velocity magnitude iso surface flow field prediction ($\theta_{S,\,front}$ = 20°, $\theta_{0,\,front}$ = 10°, $C_{T,\,front}$ = 0.031, $\theta_{0,\,rear}$ = 10°, $\theta_{S,\,rear}$ = 20°, $C_{T,\,rear}$ = 0.028).

Mars versus Earth wake flow field comparison

LILI wake and performance results are compared for Earth and Mars conditions. Nominal Earth and Mars conditions used in this study is shown in Table 3. The comparison between the two simulations in Figure 20 reveal that a higher velocity magnitude is shown for Mars conditions due to the lower density. Furthermore, the performance was compared and revealed a minimum thrust difference as shown in Table 4.

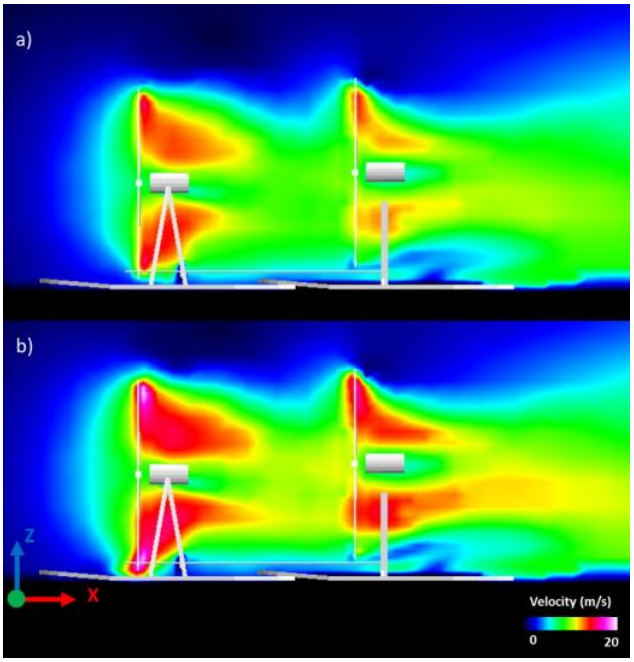

Figure 20. RotCFD velocity magnitude results for LILI in ground mode: a) Earth ($C_{T,\,front}$ = 0.0028, $C_{T,\,front}$ = 0.0017) and b) Mars conditions ($C_{T,\,front}$ = 0.0026, $C_{T,\,front}$ = 0.0015) (for Earth and Mars settings: ($\theta_{S,\,front}$ = 90°, $\theta_{0,\,front}$ = 10°,, $\theta_{S,\,rear}$= 90°, $\theta_{0,\,rear}$ = 10°).

Hover downwash performance with and without skies

The aerodynamic performance impact of the use of skis in hover is analyzed with and without skis to highlight possible limitations of the presence of the skis. Figure 21 shows LILI in hover with a velocity magnitude contour in the

X-Z plane at Y=0. Figure 22 shows the same configuration as Figure 21, but without the skis to show the change in flow field with and without the skis. Wake impingent on the ski is shown for the rear ski. The thrust of each rotor in hover is shown in Table 5 and compared to with and without skis. When the skis are present, the thrust is higher compared to without skis. Due to the suggested limited hover time necessary to complete missions, any sizing to the ski to accommodate for an improve hover performance specifically is not suggested.

Table 4. LILI ground mode rotor forward propulsive performance on Earth and Mars.

	$C_{T,\ front}$	$C_{T,\ rear}$
Earth	0.0028	0.0017
Mars	0.0026	0.0015
ΔC_T	0.0002	0.0002

Table 5. LILI hover performance with and without skis.

	$C_{T,\ front}$	$C_{T,\ rear}$
With skis	0.0253	0.0260
Without skis	0.0175	0.0203
ΔC_T	0.0078	0.0057

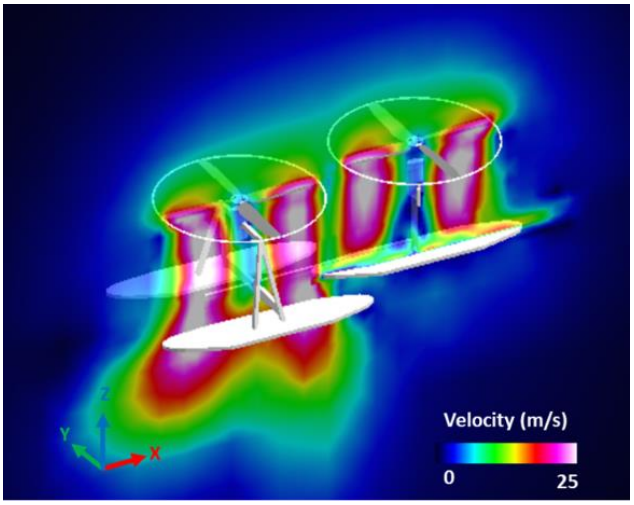

Figure 21. LILI conceptual design in hover with skis. RotCFD velocity magnitude results in the X-Z plane ($\theta_{S,\ front}$ = 0°, $\theta_{0,\ front}$ = 10°, $C_{T,\ front}$ = 0.0253, $\theta_{S,\ front}$ = 0°, $\theta_{0,\ rear}$ = 10°, $C_{T,\ rear}$ = 0.0260).

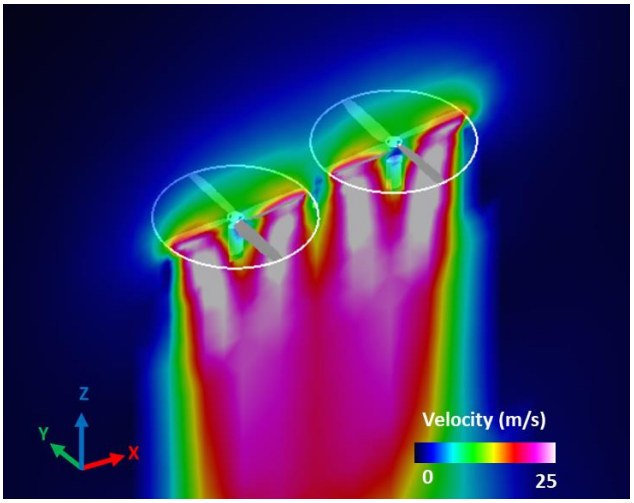

Figure 22. LILI in hover without skis. RotCFD velocity magnitude results in the X-Z plane ($\theta_{S,\ front}$ = 0°, $\theta_{0,\ front}$ = 10°, $C_{T,\ front}$ = 0.0175, $\theta_{S,\ front}$ = 0°, $\theta_{0,\ rear}$ = 10°, $C_{T,\ rear}$ = 0.0203).

Directional control: turning and backing up

LILI's control is performed using collective and cyclic control. Due to the front support structure, the use of the horizontal rotation of LILI's front rotor is limited.
The use of collective and cyclic input is used to turn and back up LILI in order to explore within the designed missions.

For LILI to turn, the use of cyclic control is implemented in each rotor. Since the front and rear rotors are rotating in opposite directions for torque balancing, an input of lateral cyclic pitch ($\theta_{1c,\ front}$) of 8° and longitudinal cyclic pitch ($\theta_{1s,\ front}$) of 8° for the front rotor and lateral cyclic pitch ($\theta_{1c,\ rear}$) of 8° and longitudinal cyclic pitch ($\theta_{1s,\ rear}$) of 8° for the rear rotor, was chosen as an example flight condition. Figure 23 shows RotUNS velocity magnitude isosurface wake results of LILI turning with the use of cyclic input. The resultant flow field reveals a force resulting in a turn-about the Z-axis due to the thrust vectors centered on opposite sides for each rotor.

The reverse, or backing up, capability of the LILI vehicle while on the ground is performed by setting a negative collective control input, see Figure 24. To move LILI backward, a negative collective input for the front and rear rotor is inputted ($\theta_{0,\ front}$, $\theta_{0,\ rear}$). The negative collective control input results in a negative thrust vector with a wake in the negative X-direction, opposite of what is shown in Figure 18.

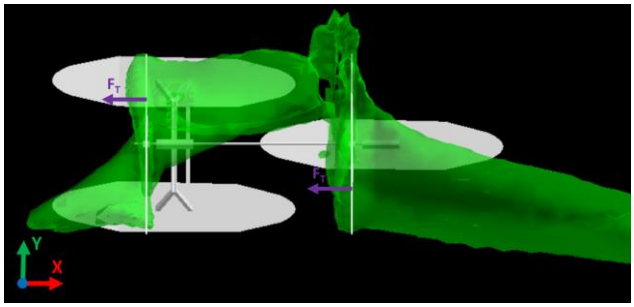

Figure 23. Top view of RotCFD flow field results of LILI turning about the Z-axis with use of cyclic input ($\theta_{S,\ front}$ = 90°, $\theta_{0,\ front}$ = 0°, $\theta_{1c,\ front}$ = 8°, $\theta_{1s,\ front}$ = 8°, $C_{T,\ front}$ = 0.0003, $\theta_{S,\ front}$ = 90°, $\theta_{0,\ rear}$ = 0°, $\theta_{1c,\ rear}$ = 8°, $\theta_{1s,\ rear}$ = 8°, $C_{T,\ rear}$ = 0.0001).

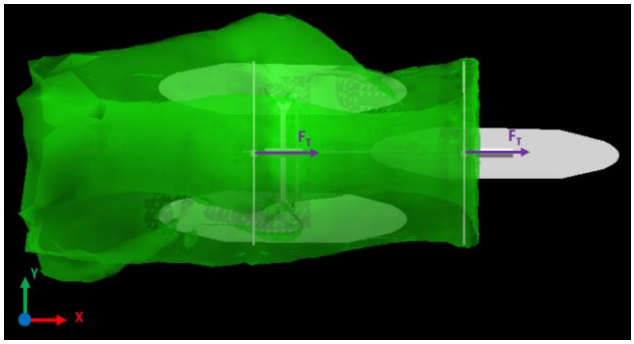

Figure 24. Top view of RotCFD flow field results of LILI backing up using collective control input ($\theta_{S,\ front}$ = 90°, $\theta_{0,\ front}$ = -10°, $C_{T,\ front}$ = -0.0029, $\theta_{S,\ front}$ = 90°, $\theta_{0,\ rear}$ = -10°, $C_{T,\ rear}$ = -0.0032).

Summary

The recent success of the Ingenuity Mars Helicopter is anticipated to result in an explosion of aerospace innovation for aerial vehicle exploration of Mars. The LILI (Long-term Ice-field Levitating Investigator) project is a hybrid aerial/ground mobility concept that is designed for ground and aerial exploration. LILI's approach is to maximize the efficiency and robustness of Martian and terrestrial field science campaigns.

Key design features have been identified that make LILI unique compared to the Mars Helicopter. This includes the use of skis and propeller-driven propulsion for ground mobility. LILI's baseline design has also been examined by modifying the original design to add the feature of a ski plus wheel configuration. The implications of ski snow/icy surface friction coefficients and minimum requirements for ski planform area were carefully considered. With these key unique ground mobility parameters identified and implemented, an initial sizing analysis was derived and discussed that leverages a previously developed Mars rotorcraft sizing spreadsheet.

Previous and/or attempted missions are summarized in this paper along with defining LILI-specific missions to utilize LILI's unique capabilities to explore the northern polar cap of Mars. Two possible locations for missions would challenge LILI with icy canyons and harsh rocky terrains, while also taking advantage of scientific experiments of interest to MEPAG.

Entry, descent, and landing (EDL) storage and deployment are considered by discussing the use of a parachute and sky crane (analogous to what was used to land the Curiosity and Perseverance rovers) to land LILI safely on the surface of Mars. LILI is stored in an aeroshell by use of collapsible/expandable telescoping tubes and/or truss structures. Future work should include more in-depth design work into EDL deployment.

An initial aerodynamic performance and controllability study work was performed by use of the RotUNS computational fluid dynamics tool. Flow field predictions of rotor wake behavior for LILI in hover, forward flight, and ground-mobility mode are presented that reveal possible wake interference (and fuselage download) issues in hover. A comparative study of the performance and flow fields of LILI on Mars and Earth is investigated that reveals a higher velocity magnitude is shown for Mars conditions due to the lower density. Initial investigation into the directional control of LILI, while on the ground, in terms of turning and backing up with the use of collective and cyclic control input, with a visualization of rotor wake behavior, is presented.

As scientists and engineers continue to pursue the exploration of Mars, new and uniquely designed aerial plus ground exploration vehicles will need to be developed. The union of an aerial plus ground exploration vehicle gives the capability to explore areas with harsh terrain and atmospheric conditions. LILI opens the doors to learn not only about polar regions of Mars but also gives engineers motivation to design outside the conventional design "box".

ACKNOWLEDGMENTS

Special thanks to Dr. William Warmbrodt, Dr. Wayne Johnson, Dr. Gloria Yamauchi, Mr. Christopher Silva, and the Aeromechanics Office for guidance and advice. Extended thanks to Dr. Wayne Johnson for providing the MSH spreadsheet.

REFERENCES

1. Squyres, S.W., Knoll, A.H., Arvidson, R.E., Ashley, J.W., Bell, J.F., Calvin, W.M., Christensen, P.R., Clark, B.C., Cohen, B.A., De Souza, P.A. and Edgar, L., "Exploration of Victoria Crater by the Mars Rover Opportunity." Science 324.5930.
2. Balaram, J.B., Canham, T., Duncan, C., Golombek, M., Grip, H.F., Johnson, W., Maki, J., Quon, A., Stern, R., and Zhu, D. "Mars Helicopter Technology Demonstrator." AIAA Paper No. 2018-0023, AIAA Science and Technology Forum and Exposition (AIAA

SciTech), Orlando, FL, January 2018.
3. Young, L. A., Aiken, E., Briggs, G., Lee, P., Pisanich, G., Withrow-Maser, S., Cummings, H., "The Future of Rotorcraft and other Aerial Vehicles for Mars Exploration," VFS 77th Annual Forum, Virtual, May 2021.
4. Banfield, D., Stern, J., Davila, A., Johnson, S.S., Brain, D., Wordsworth, R., Horgan, B., Williams, R.M., Niles, P., Rucker, M. and Watts, K. "Mars Science Goals, Objectives, Investigations, and Priorities: 2020 Version", Mars Exploration Program Analysis Group, 2020. https://mepag.jpl.nasa.gov/reports/MEPAGGoals_2020_MainText_Final.pdf
5. Drake, Nadia. "Why We Explore Mars-and What Decades of Missions Have Revealed." *Science*, National Geographic, 4 May 2021.
6. Fastook, J. L. & Head, J. W. III Early Mars climate near the Noachian–Hesperian boundary: Independent evidence for cold conditions from basal melting of the south polar ice sheet (Dorsa Argentea Formation) and implications for valley network formation. Icarus 219, 25–40 (2012).
7. Masursky, H., An overview of geologic results from Mariner 9, J. Geophys. Res., 78, 4009-4030, 1973.
8. Hoffman, J. H.; Chaney, R. C.; Hammack, H. Phoenix Mars Mission— The Thermal Evolved Gas Analyzer. J. Am. Soc. Mass Spectrom. 2008, 19, 1377–1383.
9. Cull, S. C. et al. Concentrated perchlorate at the Mars Phoenix landing site: Evidence for thin film liquid water on Mars. Geophys. Res. Lett. 37, L22203 (2010).
10. Koning, W. J. F., Johnson, W., Grip, H., "Improved Mars Helicopter Aerodynamic Rotor Model for Comprehensive Analyses," Presented at the 44th European Rotorcraft Forum, Delft, the Netherlands, 18-21 September 2018.
11. Hao, S., and Su, J., "Basic Snow Pressure Calculation." 4th International Conference on Advanced Engineering and Technology, Vol. 317. No. 1., 2018.
12. Johnson, W., Withrow-Maser, S. Young, L., Malpica, C., Koning, W., Kuang, W., Fehler, M. Tuano, A., Chan, A., Datta, A. Cheng, C., Lumba, R., Escobar, E., Balaram, J., Tzanetos, T., and Grip, H.F., "Mars Science Helicopter Conceptual Design." NASA TM 2020-220485, March 2020.
13. Albee, A., Battel, S., Brace, R., Burdick, G., Casani, J., Lavell, J., Leising, C., MacPherson, D., Burr, P. and Dipprey, D. (2000). Report on the Loss of the Mars Polar Lander and Deep Space 2 Missions. JPL Special Review Board, Jet Propulsion Lab (JPL).
14. Law, E., and Day, B. (2017). Mars trek: An interactive web portal for current and future missions to Mars. In European Planetary Science Congress (Vol. 11, pp. EPSC2017–99).
15. Thomas, P.C., Malin, M.C., Edgett, K.S., Carr, M.H., Hartmann, W.K., Ingersoll, A.P., James, P.B., Soderblom, L.A., Veverka, J. and Sullivan, R., "North-south geological differences between the residual polar caps on Mars", Nature, 404, 161-164, 2000.
16. Zacny, K. and Cooper, G. (2006c) Considerations, constraints and strategies for drilling on Mars. Planet. Space Sci. 54:345–356.
17. Zacny, K. and Cooper, G. (2007b) Methods for cuttings removal from holes drilled on Mars. MARS 3:1–11 (doi: 10.1555/ mars.2007.0001).
18. Gupta, R. N., Lee, K. P., and Scott, C. D., "Aerothermal Study of Mars Pathfinder Aeroshell," *Journal of Spacecraft and Rockets*, Vol. 33, No. 1, 1996, pp. 61–69.
19. Nelessen, A., Sackier, C., Clark, I., Brugarolas, P., Villar, G., Chen, A., Stehura, A., Otero, R., Stilley, E., Way, D. and Edquist, K., "Mars 2020 Entry, Descent, and Landing System Overview," Proc. IEEE Aerospace Conference, March 2019.
20. Rajagopalan, R. G., Baskaran, V., Hollingsworth, A., Lestari, A., Garrick, D., Solis, E., and Hagerty, B., "RotCFD A Tool for Aerodynamic Interference of Rotors: Validation and Capabilities," American Helicopter Society Aeromechanics Specialists Conference, San Francisco, CA, January 18-20, 2012.
21. Guntupalli, K., Novak, L. A., and Rajagopalan, R. G., "RotCFD: An Integrated Design Environment for Rotorcraft," American Helicopter Society Aeromechanics Specialists Conference, San Francisco, CA, January 20-22, 2016.